LAWRENCE
LIVERMORE
NATIONAL
LABORATORY

LLNL-PROC-680591

Simulations and Experiments of the Growth of the "Tent" Perturbation in NIF Ignition Implosions

B. A. Hammel, R. Tommasini, D. S. Clark, J. Field, M. Stadermann, C. Weber

January 7, 2016

IFSA
Seattle, WA, United States
September 20, 2015 through September 25, 2015

Disclaimer

Simulations and Experiments of the Growth of the "Tent" Perturbation in NIF Ignition Implosions

B.A. Hammel, R. Tommasini, D.S. Clark, J. Field, M. Stadermann, C. Weber

[1]Lawrence Livermore National Laboratory, CA, USA

hammel1@llnl.gov

Abstract. NIF capsules are supported in the hohlraum by two thin (~15-110 nm) Formvar films ("tent"). Highly resolved HYDRA simulations indicate that a large (~40% peak-average) areal density (ρR) perturbation develops on the capsule during acceleration as a consequence of this support geometry. This perturbation results in a jet of dense DT and, in some cases, CH that penetrates and cools the hot spot, significantly degrading the neutron yield (~10-20% of 1D yield). We examine "low-foot" and "high-foot" pulse shapes, tent thicknesses, and geometries. Simulations indicate that thinner tents result in a smaller ρR perturbation, however, the departure angle of the tent from the capsule surface is important, with steeper angles resulting in larger perturbations.

1. Tent geometry

NIF capsules are supported in the hohlraum by two thin (~15-110 nm) Formvar films ("tent") that are stretched over the two poles of the capsule and supported at the joint between the upper and lower halves of the hohlraum [1][2][3]. Metrology of the assembled targets (See insert in Figure 1) indicates that a 50-nm-thick tent follows the curvature of the capsule for ~ 40° (measured from the pole), and then departs from the capsule at an angle that is ~15° steeper than tangential (i.e. 15° "off-tangent" (OT) angle). The angle continues to increase as the distance from the capsule surface increases. The tent angle likely varies azimuthally around the capsule since the tent support is affected in areas near diagnostic holes in the hohlraum. Recent measurements indicate that the departure angle depends on tent thickness, with thinner tents having steeper departure angles. These measurements are made for capsules at room temperature. Measurements of targets at cryogenic temperatures, where the tent angle could be affected, are in progress.

2. Simulation Method

Direct numerical simulations of the impact of the tent on NIF ignition target designs are difficult due to the challenge of resolving the tent thickness. Typical high-resolution simulations without a tent have a radial zone spacing of ~40 nm in the outer ablator region (~ 1 g/cm^3), and ~400 nm in the surrounding gas (~1 mg/cm^3). Fully resolving the tent (~ 5 zones across a 50 nm thick tent) implies ~10 nm zones in the gas and therefore ~1 nm zones in the denser ablator. Such fine radial zoning sets a limit on the angular zoning due to zone aspect ratio limits and run stability. Tent simulations reported here have ~ 5000 radial zones and 5120 angular zones (over 90°). The small zone size limits the Courant time step to impractically long run times. The strategy taken here is to rezone the ablated region after the tent has exploded, at ~ 1 ns after the start of the drive. Lower resolution simulations where the tent is under-resolved (e.g. 1 zone across the tent), or modeled at lower density and

increased thickness (ρR constant), have shown qualitatively similar results, but with differences in the details of the resulting perturbation. In the simulations reported here we approximate the tent geometry and assume the tent departs the capsule at a fixed OT angle (i.e. the tent follows the curvature of the capsule and then departs in a straight line). These simulations are of the capsule and tent only, using an x-ray drive taken from integrated capsule-hohlraum simulations. The impact of the tent with other sources of perturbation included (e.g. surface roughness, drive asymmetry, fill-tube, etc.) has been assessed in lower resolution simulations that use an "equivalent" surface perturbation that match the ρR perturbation from the high-resolution simulations reported here.[4]

3. Tent seeded perturbation

The interaction of the tent with the capsule is complex. The departure of the tent from the capsule surface leads to a small jump in areal density $\rho R/\langle \rho R \rangle \sim 10^{-5}$, which increases with increasing OT angles. This ρR perturbation is small (0.1x) compared to typical capsule surface perturbations, and should be negligible. However, as the tent explodes and collides with the ablating capsules material, a pressure wave is created that propagates in the polar direction away from the contact point towards the equator. Resulting Kelvin-Helmholtz growth may create a seed for further hydrodynamic growth. In addition, as the tent explodes the gradient in the density of the ablated capsule material is misaligned with the gradient in the pressure from the exploding tent, creating vorticity in the ablated region $\omega \sim -\nabla P \times \nabla \rho \sim |\nabla P| \cdot |\nabla \rho| \cdot \sin(\theta)$. The induced vorticity increases with increasing OT angle. The perturbation seeded by these processes is then amplified by Rayleigh-Taylor (R-T) when the capsule accelerates inward.

4. Simulations and Experiments

The simulated fractional areal density perturbation $\rho R/\langle \rho R \rangle$, near the time of peak implosion velocity, resulting from a 50-nm-thick tent on a CH Symcap driven with a "low-foot" (LF) drive, for a range of OT angles, is shown in Figure 1. [5][6] The tent perturbation increases markedly with increasing OT angle, reaching a level of +35% to -40% peak-to-valley. Results for a "high-foot" (HF) drive [7], for the 0° OT angle case is also shown.

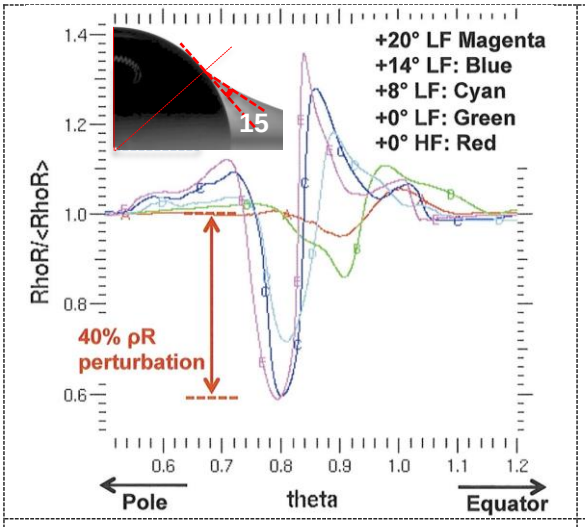

Figure 1. $\rho R/\langle \rho R \rangle$ *vs.* theta (rad) for different OT angle. Insert shows a pre-shot image of capsule and tent. Tent departs with ~15° OT angle. Simulations: Symcap targets.

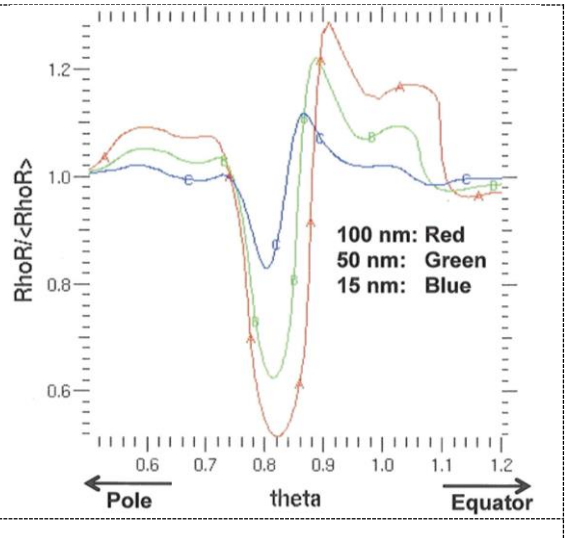

Figure 2. $\rho R/\langle \rho R \rangle$ *vs.* theta (rad) for different tent thickness. All with 14° OT angle and LF drive. Simulations: DT targets.

Simulations show that the perturbation for the HF case is slightly larger than LF after shock transit and prior to capsule acceleration, but the larger R-T growth for the LF case leads to a perturbation that is ~ 2.5x larger than HF. The simulated $\rho R/\langle \rho R \rangle$ for different tent thicknesses on CH DT targets (N120321), all with 14° OT angle, is shown in Figure 2. Thinner tents result in a smaller perturbation.

The ρR perturbation (Peak-to-Average) of implosions, near peak velocity (200 μm radius), are shown in Figures 3 [8] and 4. In Figure 3, pluses are the *actual* ρR perturbation from the simulations shown in Figure 1 (Symcap implosions). In Figure 4, pluses are the *actual* ρR perturbation from the simulations of DT implosions shown in Figure 2, and the open circle (for 50 nm thickness case) is for the equivalent Symcap target. The close agreement indicates that the ρR perturbation at peak velocity resulting from a given tent thickness is nearly identical for Symcap and DT implosions. In Figures 3 and 4, solid circles are *inferred* values of ρR perturbation from simulated x-ray radiographs at perfect resolution (see insert).[8] The excellent agreement with *actual* ρR perturbation from simulations (pluses) validates the unfold method used to infer ρR from radiographic transmission through the capsule $e^{-\kappa \rho L}$.[8] Squares are inferred ρR perturbation from simulated radiographs, blurred to match the experimental resolution (20 μm). In Figure 3, inferred values from experimental measurements of LF implosions fall in the range marked in blue, implying OT angles of 8-16°, generally consistent with pre-shot metrology. Note: the inferred values of 15%, at the 20 μm experimental resolution, imply *actual* ρR perturbations of ~30-40%. For HF implosions, the inferred perturbation is consistent with an actual ρR perturbation of ~5%. Figure 4 shows the inferred ρR perturbation from simulations for different tent thicknesses, all with 14° OT angle, and experimental measurements for LF implosions. The values inferred from simulations (20 μm resolution) and those inferred from experimental radiographic measurements, for LF implosions, are in good agreement except at the largest tent thicknesses. This may be due to a decrease in the tent's OT angle with increasing tent thicknesses. Inferred ρR perturbation from measurements on HF implosions is also shown. Simulations are in progress for this case.

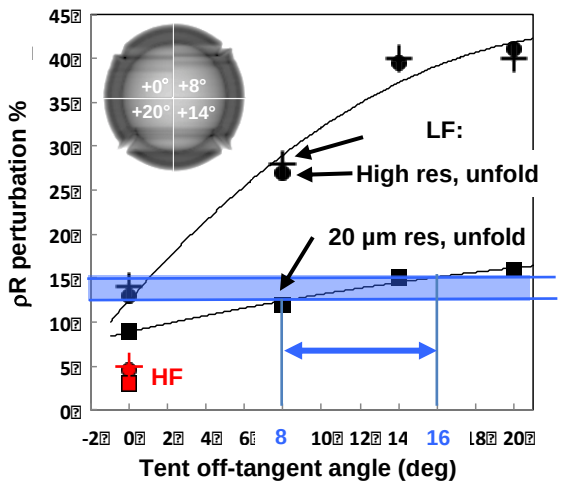

Figure 3. Areal density (ρR) perturbation (Peak-to-Average) *vs.* tent departure angle. Black: LF drive, Red: HF drive. Insert: Simulated radiographs for different OT angle from LF drive, Symcap implosions.

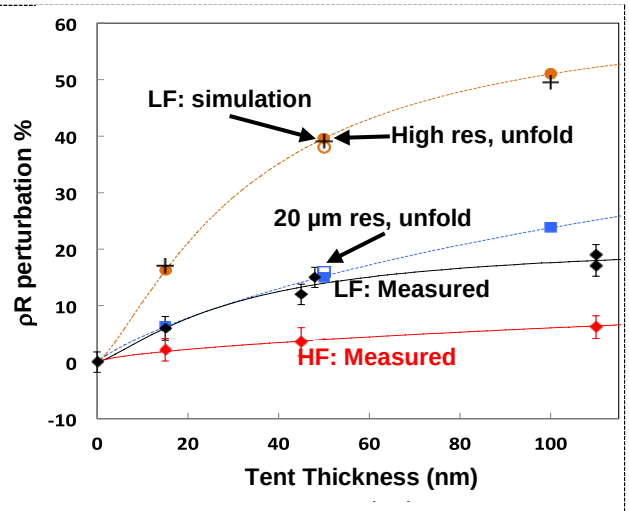

Figure 4. ρR perturbation (Peak-to-Average) *vs.* tent thicknesses. All with 14° OT angle. Black: LF drive, Red: HF drive. Closed circles and squares: DT implosion. Open circles and squares: Symcap implosion. Measurements: Symcap implosions.

As the capsules continue to compress, simulations indicate that the perturbation resulting from the tent has a significant impact on the hot-spot shape, and the resulting performance. Figure 5 shows density and temperature at peak compression for a DT target (N120321), driven with a LF pulse, with a 50-nm-thick tent at 14° OT angle. The region of low ρR results in escaping hot-spot mass, and the

regions of high ρR result in a jet of cold DT (~1 μg) penetrating the hot-spot, causing local cooling. The resulting x-ray hot-spot shape has a strong (P_4/P_0 ~ 30%) distortion (Figure 6), in qualitative agreement with experiments.[9] For a 50-nm-thick tent, and no other sources of perturbation, the neutron yield is degraded to 18% of the 1D value. Although no CH enters the hot-spot in this case, simulations of N120321 that include drive asymmetry and a 100-nm-thick tent (n.b. tent on this shot was 110 nm) indicate that 1.5 μm of CH and 4 μg of cold DT enter the hot-spot.

We are exploring thinner tents and alternate mounting schemes. Simulations indicate that for a 15-nm-thick tent the ρR perturbation (Figure 4) and resulting jet are reduced. With only this perturbation, the neutron yield is degraded to 58% of the 1D value. Alternate mounting schemes under development include "polar-contact" tents that reduce the solid angle of the perturbation and the resulting mix.

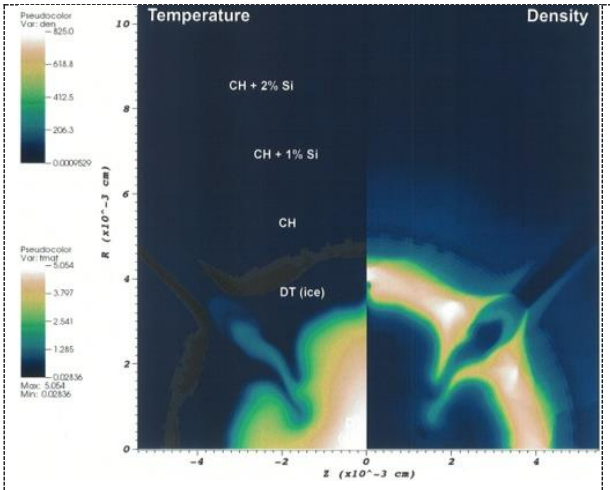

Figure 5. Simulation of DT target implosion near peak compression, driven by LF pulse, with 50-nm-thick tent at 14° OT angle. Right Frame: Density. Left Frame: Temperature. The tent perturbation results in a jet of cold DT that penetrates the hot-spot.

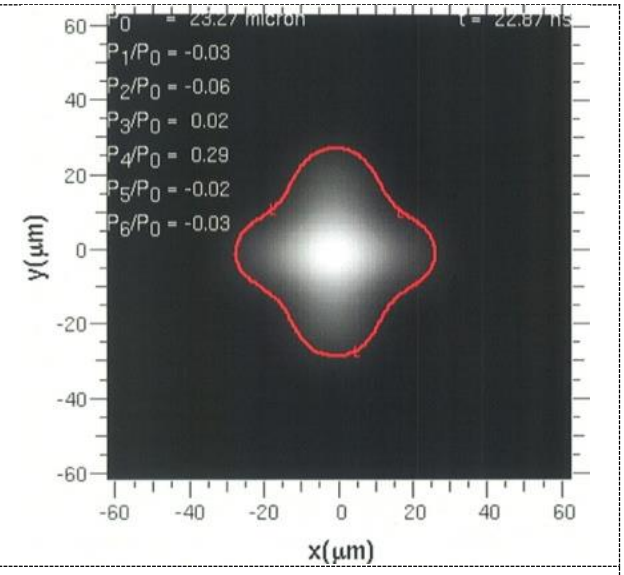

Figure 6. Simulated x-ray image. Legendre polynomial fit (15% contour) indicates a ~30% P_4/P_0 distortion.

References

[1] Baxamusa S H, et al., Langmuir **30**, 5126 (2014).
[2] Stadermann M, Letts S A, and Bhandarkar S, Fusion Sci. Technol. **59**, 58 (2011).
[3] Haan S W, Atherton J, Clark D S, and Hammel B A, Fusion Sci. Ignition **63**, 67–75 (2013).
[4] Clark D S et al., Physics of Plasmas, 2015. **22**(2).
[5] Lindl J, et al., Phys. Plasmas **21**, 129902 (2014)
[6] Capsule parameters and drive similar to shot N120321.
[7] Hurricane O A, et al., Nature **506,** 343–348 (2014).
[8] Tommasini R et al., Physics of Plasmas **22** (5), 2015.
[9] Nagel S R, et al., Phys. Plasmas **22**, 022704 (2015).

This work was performed under the auspices of the U.S. Department of Energy by Lawrence Livermore National Laboratory under Contract No. DE-AC52-07NA27344